Available online at www.sciencedirect.com
SCIENCE DIRECT®
Journal of Molecular Catalysis A: Chemical 210 (2004) 197–204
JOURNAL OF MOLECULAR CATALYSIS A: CHEMICAL
www.elsevier.com/locate/molcata

A spectroscopic study on the reaction-controlled phase transfer catalyst in the epoxidation of cyclohexene

Jinbo Gao [a], Yangying Chen [a], Bo Han [a], Zhaochi Feng [a], Can Li [a,*], Ning Zhou [b], Shuang Gao [b], Zuwei Xi [b]

[a] *State Key Laboratory of Catalysis, Dalian Institute of Chemical Physics, Chinese Academy of Sciences, 457 Zhongshan Road, Dalian 116023, China*
[b] *Dalian Institute of Chemical Physics, Chinese Academy of Sciences, 457 Zhongshan Road, Dalian 116023, China*

Received 9 June 2003; received in revised form 19 September 2003; accepted 20 September 2003

Abstract

The epoxidation of cyclohexene with hydrogen peroxide in a biphase medium ($H_2O/CHCl_3$) was carried out with the reaction-controlled phase transfer catalyst composed of quaternary ammonium heteropolyoxotungstates $[\pi\text{-}C_5H_5N(CH_2)_{15}CH_3]_3[PW_4O_{16}]$. A conversion of about 90% and a selectivity of over 90% were obtained for epoxidation of cyclohexene on the catalyst. The fresh catalyst, the catalyst under reaction conditions and the used catalysts were characterized by FT-IR, Raman and ^{31}P NMR spectroscopy. It appears that the insoluble catalyst could degrade into smaller species, $[(PO_4)\{WO(O_2)_2\}_4]^{3-}$, $[(PO_4)\{WO(O_2)_2\}_2\{WO(O_2)_2(H_2O)\}]^{3-}$, and $[(PO_3(OH))\{WO(O_2)_2\}_2]^{2-}$ after the reaction with hydrogen peroxide and becomes soluble in the $CHCl_3$ solvent. The active oxygen in the $[W_2O_2(O_2)_4]$ structure unit of these soluble species reacts with olefins to form the epoxides and consequently the corresponding W–Ob–W (corner-sharing) and W–Oc–W (edge-sharing) bonds are formed. The peroxo group $[W_2O_2(O_2)_4]$ can be regenerated when the W–Ob–W and W–Oc–W bonds react with hydrogen peroxide again. These soluble species lose active oxygen and then polymerize into larger compounds with the W–Ob–W and W–Oc–W bonds and then precipitate from the reaction solution after the hydrogen peroxide is consumed up. Part of the used catalyst seems to form more stable compounds with Keggin structure under the reaction conditions.

Keywords: Reaction-controlled phase transfer catalysis; Epoxidation; Cyclohexene; Polyoxometalates (POMs); Biphasic catalytic system

1. Introduction

Epoxidation of olefins is among the most important reactions in organic synthesis, because epoxide compounds are valuable precursors for the synthesis of drugs, agrochemicals and food additives. Polyoxometalates, as the effective catalysts for epoxidation, have drawn wide attention in the last two decades [1–40]. The most significant developments were made in the 1980s by the groups of Venturello [13–18] and Ishii [19–25], who found that the heteropolyoxotungstophosphates show high activity and selectivity for the epoxidation of olefins and the epoxidation mechanism on these catalysts have been investigated by many groups later [26–30,39,40]. Xi et al. [38] reported a reaction-controlled phase transfer catalyst composed of quaternary ammonium heteropolyoxotungstates, $[\pi\text{-}C_5H_5N(CH_2)_{15}CH_3]_3[PW_4O_{16}]$, which is active and selective for epoxidation of propylene and other olefins (such as linear terminal olefins, internal olefins, cyclic olefins, styrene, and allyl chloride) with 30% hydrogen peroxide. This catalyst is an insoluble solid and can dissolve into the reaction solution when it reacts with hydrogen peroxide, and the catalyst becomes insoluble solid and precipitate again after the epoxidation reaction is over. Therefore, the catalyst can be easily separated from the reaction system, thus providing a approach to resolve the separation difficulty in homogeneous catalysis.

However, the mechanism of the reaction-controlled phase transfer of this catalyst is not clear. To understand the behaviors of the catalyst dissolves and precipitates in the reaction system by the reaction with hydrogen peroxide, and to identify the structural changes of the catalyst during and after the epoxidation reaction, the fresh catalyst, the catalyst under reaction conditions and the used catalysts were

* Corresponding author. Tel.: +86-411-4379070; fax: +86-411-4694447.
E-mail address: canli@dicp.ac.cn (C. Li).
URL: http://www.canli.dicp.ac.cn.

1381-1169/$ – see front matter © 2003 Elsevier B.V. All rights reserved.
doi:10.1016/j.molcata.2003.09.018

characterized by FT-IR, Raman and ^{31}P NMR spectroscopy. It is found that the reaction-controlled phase transfer is essentially a process of degradation and polymerization of the catalyst.

2. Experimental

2.1. Preparation of $[\pi$-$C_5H_5N(CH_2)_{15}CH_3]_3[PW_4O_{16}]$

The catalyst was prepared according to the procedure described previously [16,37]. A suspension of tungstic acid 2.5 g (10 mmol) in 7 ml of aqueous H_2O_2 (35%) was stirred and heated to 60 °C until a colorless solution was obtained. This solution was filtered and then cooled to room temperature. Forty percent (w/v) H_3PO_4 (0.62 ml, 2.5 mmol) was added to the solution, and then was diluted to 30 ml with water. An amount equal to 1.80 g of cetylpyridiniumammonium chloride (5 mmol) in dichloromethane (40 ml) was added dropwise with stirring in 2 min, and the stirring was continued for an additional 15 min. The organic phase was then separated, dried with anhydrous Na_2SO_4, filtered and evaporated under atmospheric pressure at 50–60 °C (bath) and about 2.5 g (85%, based on the quaternary ammonium salt charged) of the dried yellow powder was obtained by further evacuation.

2.2. Biphasic catalytic epoxidation of cyclohexene

A round-bottomed flask was charged with the catalyst (0.05 g), 35% H_2O_2 (8.0 mmol), cyclohexene (16.0 mmol), and 16 ml of $CHCl_3$. The flask was then placed in a water bath at 35 °C with vigorous stirring for 4 h. After the reaction was over, the resulting organic layer was analyzed by GC with the internal standard method. The precipitated catalyst was separated by centrifugation.

2.3. Raman spectra of the course of the catalyst preparation

During the course of the catalyst preparation, the pertungstic acid aqueous solution, the reaction solution of pertungstic acid and H_3PO_4 and the obtained solid catalyst $[\pi$-$C_5H_5N(CH_2)_{15}CH_3]_3[PW_4O_{16}]$ were, respectively, characterized by visible Raman spectroscopy (with the excitation laser at 532 nm). In the meantime, for the assignment of the Raman bands of the catalyst, cetylpyridiniumammonium chloride was measured by UV Raman spectroscopy (with the excitation laser at 325 nm), which can avoid the fluorescence interference and give a better signal-to-noise ratio than in the visible region.

UV Raman spectra were recorded on a homemade UV Raman spectrograph [41,42], visible Raman spectra were obtained on a Jobin-Yvon U1000 scanning double monochromator with the spectrum resolution of 4 cm^{-1} using a laser at 532 nm as the excitation source. Solid samples were mounted on a disk rotating at about 1000 hertz in order to avoid thermal decomposition by the laser beam.

2.4. FT-IR spectra of reaction solution

A round-bottomed flask was charged with the catalyst (0.1 g), 35% H_2O_2 (8.0 mmol), and $CHCl_3$ (16.0 ml). The reaction system was maintained at 35 °C with vigorous stirring until the system gradually changes from turbid to clear, namely, until the catalyst completely dissolves into the reaction medium. A small amount of reaction organic solution was dropped into a standard sodium chloride cell and immediately measured by FT-IR.

Infrared spectra were recorded on a Nicolet Impact 410 FT-IR spectrometer. The catalyst was measured using 2–4% (w/w) KBr pellets and prepared by manual grinding using a mortar and pestle, and the spectra of solution were recorded with a standard sodium chloride cell.

2.5. ^{31}P NMR spectra of reaction solution

A round-bottomed flask was charged with catalyst (0.1 g), 35% H_2O_2 (8.0 mmol), and $CHCl_3$ (16.0 ml). The reaction system was maintained at 35 °C with vigorous stirring until the system gradually changes from turbid to clear, and then the reaction organic solution sample was taken and immediately measured by ^{31}P NMR. Then the substrate cyclohexene was added into the reactor, the mixture was maintained at 35 °C with vigorous stirring for 30 min., organic solution from the reaction system then quickly analyzed by ^{31}P NMR again.

^{31}P NMR spectra were recorded at 9.4 T on a Bruker DRX 400 spectrometer. The ^{31}P MAS NMR spectra of solid catalyst with high-power proton decoupling were performed at 161.9 MHz with BBO MAS probe head using 4 mm ZrO_2 rotors and 2.0 μs pulse and 2 s repetition time and 2048 scans, with samples spun at 8 kHz and referenced to 85% H_3PO_4. The ^{31}P NMR spectra of the catalyst in solvents were obtained with BBI 5 mm converse phase broadband probe head using real sample solution with D_2O internal tube locking field.

3. Results and discussion

3.1. Epoxidation of cyclohexene in a biphase medium

In this study, cyclohexene was chosen as a model substrate to test the catalytic activities of the fresh and the reused catalysts. In order to ensure all of the hydrogen peroxide is consumed up, the excess olefin is necessary for the catalyst to precipitate from the reaction medium in the end of the reaction. The catalyst can be recovered easily from the reaction media by a simple filtration after the reaction, and the recovered catalyst was used again for the comparison with

Table 1
Epoxidation of cyclohexene on the catalyst $[\pi\text{-}C_5H_5N(CH_2)_{15}CH_3]_3[PW_4O_{16}]$ for different cycles

	Conversion (%)	Selectivity (%)
Fresh catalyst	95	97
Used catalyst	94	96

Reaction conditions: cyclohexene (16.0 mmol); catalyst:H_2O_2:cyclohexene = 1:300:600 (molar ratio); 16 ml of $CHCl_3$ at 35 °C for 4 h. The conversion of cyclohexene was based on H_2O_2 and the selectivity to cyclohexene oxide was based on cyclohexene.

the fresh catalyst. The reaction results of the fresh catalyst and the reused one are summarized in Table 1, for the fresh catalyst, the conversion is about 95% based on hydrogen peroxide and the selectivity is about 97% for cyclohexene, it appears that the catalytic activity and selectivity of the reused catalyst slightly decreases under the reaction conditions.

3.2. Characterization of the fresh catalyst

In order to better understand the structural changes of the catalyst during the preparation, the catalyst samples derived in the process of preparation were characterized by Raman spectroscopy. The yellow solid tungstic acid was dissolved in excess H_2O_2 to form colorless pertungstic acid [14]. The Raman spectra of pertungstic acid $[W_2O_3(O_2)_4(H_2O)_2]^{2-}$ in solution with H_2O_2 (see Fig. 1a) shows characteristic bands at 314, 560, 854, and 962 cm^{-1}, and these bands can be assigned to ν(W–O_2H), ν[W(O_2)], ν(O–O), and ν(W=O), respectively [9,26]. The band at 875 cm^{-1} is due to the ν(O–O) of hydrogen peroxide [26]. Fig. 1b shows the Raman spectrum of the reaction aqueous solution of pertungstic acid and H_3PO_4, which gives the same Raman bands as pertungstic acid, while the band of the bridging anion PO_4^{3-} are not clearly observed. The UV Raman spectra of cetylpyridiniumammonium chloride is given in Fig. 1c, strong bands are observed at 648 and 1028 cm^{-1}. Fig. 1d exhibits the Raman bands at 314, 560, 648, 854, 880, 962, and 1028 cm^{-1} of the fresh catalyst. Comparing Fig. 1d with Fig. 1b and c, the Raman bands at 314, 560, 854, and 962 cm^{-1} can be attributed to ν(W–O_2H), ν[W(O_2)], ν(O–O), and ν(W=O), respectively [9,26]. And the two bands at 648 and 1028 cm^{-1} are easily attributed to the quaternary cations.

The FT-IR spectrum of the fresh catalyst (see Fig. 2a or Fig. 3a) gives eight bands at 543, 684, 716, 775, 813, 884, 935, and 1079 cm^{-1} in the fingerprint region. The strong and broad bands at 1079 and 935 cm^{-1} can be ascribed to the stretching mode of the P–O bond and the W=O bond, respectively [16]. Based on the survey of the literature [43–45], the IR band at 884 cm^{-1} and the weak band at 813 cm^{-1} can be attributed to the ν(W–Ob–W) (corner-sharing), and ν(W–Oc–W) (edge-sharing), respectively [43–45]. The bands at 775, 716, 684 cm^{-1} are due to the quaternary cation. In addition, it can be seen that the ν(O–O) band disappears in IR spectrum, but still exists in the Raman spectra, indicating that the symmetry of the local structure with O–O bond makes this band Raman active, but infrared inactive. The ^{31}P MAS NMR spectrum of the fresh catalyst (see Fig. 4a) gives several broad peaks and suggests that the catalyst is a mixture that contain several different polytungstophosphate species.

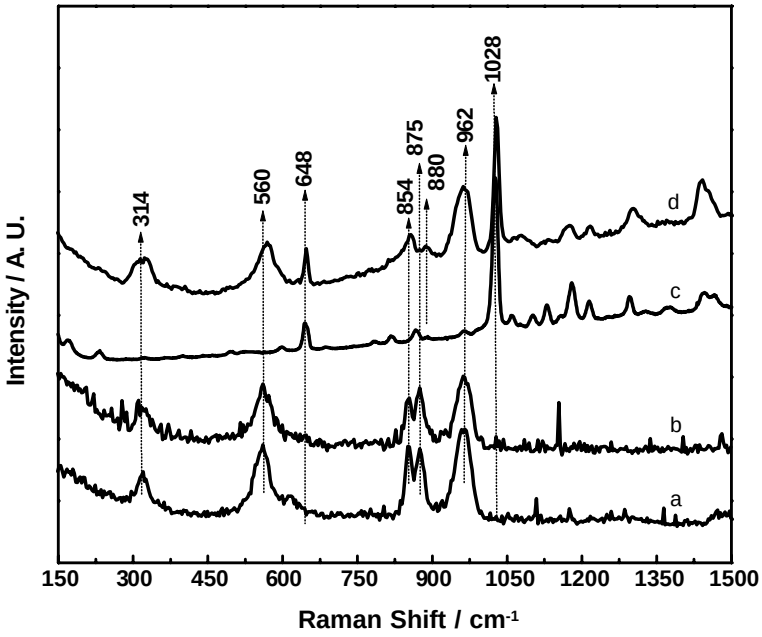

Fig. 1. Raman spectra of the course of the catalyst $[\pi\text{-}C_5H_5N(CH_2)_{15}CH_3]_3[PW_4O_{16}]$ preparation: (a) $H_2WO_4 + H_2O_2$; (b) $H_2WO_4 + H_2O_2 + H_3PO_4$; (c) cetylpyridiniumammonium chloride; (d) the fresh catalyst $[\pi\text{-}C_5H_5N(CH_2)_{15}CH_3]_3[PW_4O_{16}]$.

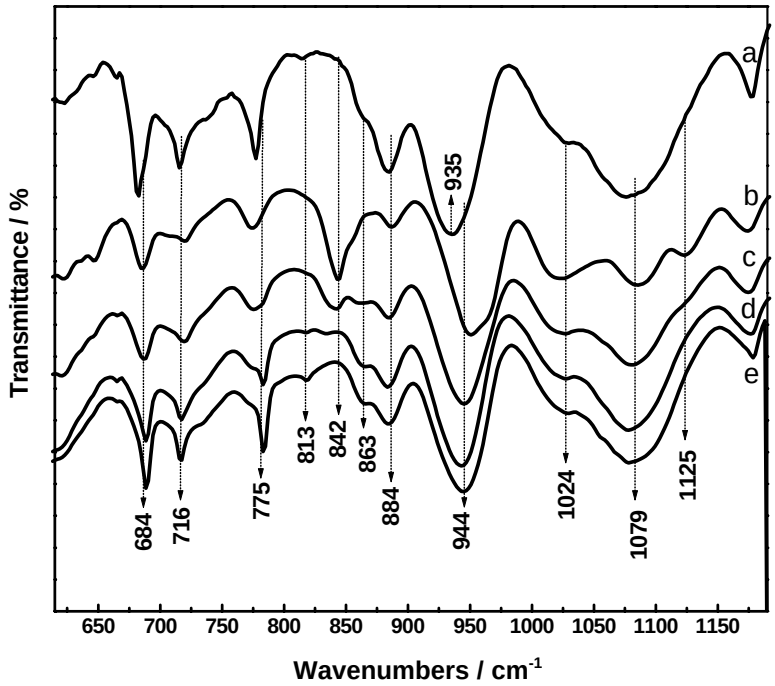

Fig. 2. FT-IR spectra of the catalyst $[\pi\text{-}C_5H_5N(CH_2)_{15}CH_3]_3[PW_4O_{16}]$ under reaction conditions: (a) the fresh solid catalyst $[\pi\text{-}C_5H_5N(CH_2)_{15}CH_3]_3[PW_4O_{16}]$; (b) the taken solution sample recorded at 1 min; (c) the taken solution sample recorded at 5 min; (d) the taken solution sample recorded at 10 min; (e) the taken solution sample recorded at 20 min.

3.3. Characterization of the catalyst under reaction conditions

To study the behaviors of the active species and to clarify the mechanism of reaction-controlled phase transfer of the catalyst, the reaction solution with catalyst is characterized by FT-IR and ^{31}P NMR during the reaction course. Fig. 2b–e displays the IR spectra of the taken solution sample recorded at 1, 5, 10, and 20 min, respectively. The characteristic bands of the catalyst at 684, 716, 775, 842, 884, 944, and 1024–1125 cm^{-1} are observed in Fig. 2b. This spectrum is similar to that reported by Venturello and D'Aloisio

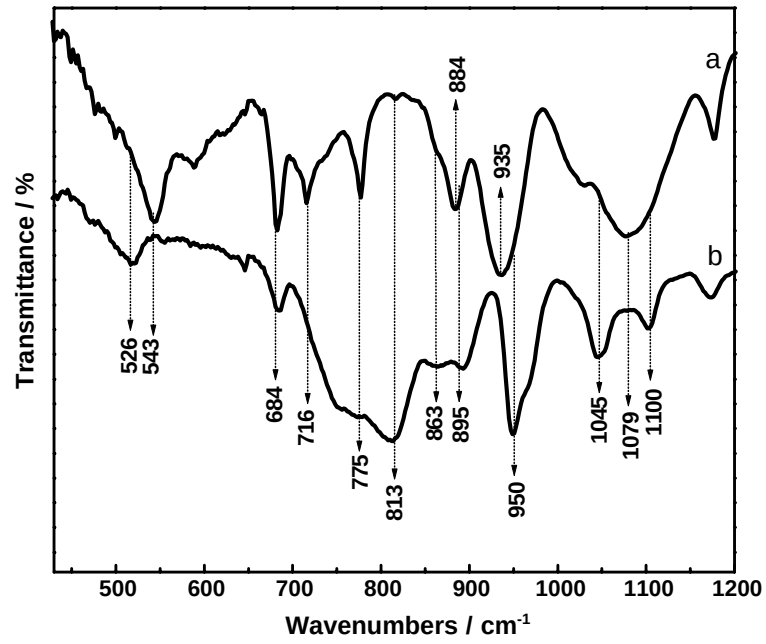

Fig. 3. FT-IR spectra of the used catalyst: (a) the fresh catalyst $[\pi\text{-}C_5H_5N(CH_2)_{15}CH_3]_3[PW_4O_{16}]$; (b) the used catalyst.

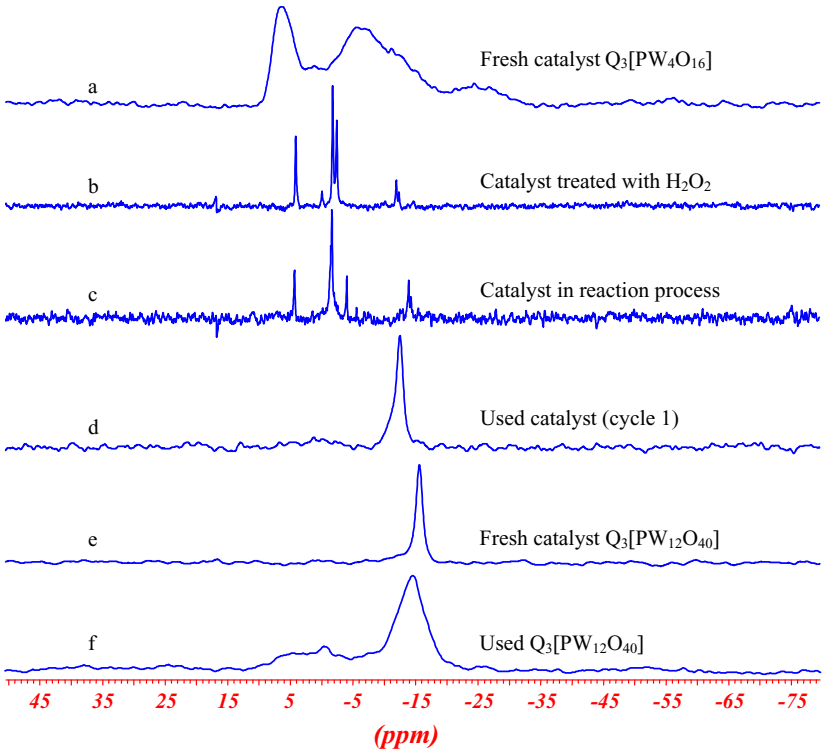

Fig. 4. ^{31}P NMR spectra of: (a) the fresh catalyst [π-$C_5H_5N(CH_2)_{15}CH_3]_3[PW_4O_{16}]$; (b) the catalyst treated with H_2O_2; (c) the catalyst in reaction process; (d) the used catalyst; (e) the fresh catalyst [π-$C_5H_5N(CH_2)_{15}CH_3]_3[PW_{12}O_{40}]$; (f) the used catalyst [π-$C_5H_5N(CH_2)_{15}CH_3]_3[PW_{12}O_{40}]$.

[16] with the exception that the weak band at 884 cm^{-1} is different. The IR bands at 1024–1125, 932, and 842 cm^{-1} can be assigned to ν(P–O), ν(W=O), and ν(O–O), respectively [16]. Other three bands at 775, 716, and 684 cm^{-1} are due to the quaternary cation. Comparing the IR spectra of the fresh catalyst treated with hydrogen peroxide with the IR results of the fresh catalyst (see Fig. 2a), the broad band at 1079 cm^{-1} in the P–O vibrational region splits into two bands at 1024 and 1125 cm^{-1}, moreover, the intensity of the ν(W–Ob–W) band at 884 cm^{-1} decreases and the band of ν(O–O) at 842 cm^{-1} appears. The results show that the catalyst obtains the active oxygen via the reaction with hydrogen peroxide.

Comparing the spectra in Fig. 2b–e, with the increase of the time intervals for recording the spectrum, obvious changes in the ν(O–O) region of the catalyst are observed. The ν(O–O) band at 842 cm^{-1} declines dramatically with the appearance of a new band at 863 cm^{-1}, meanwhile, accompanying with the growth in the intensity of the band at 884 cm^{-1}. While the further increase of time to about 10 min, another new band at 813 cm^{-1} appears (Fig. 2d). This result demonstrates that the catalyst loses the active oxygen easily in the absence of hydrogen peroxide. IR spectra show that the appearance of the bands at 884, 863 and 813 cm^{-1} is related to the gradual disappearance of the ν(O–O) band at 842 cm^{-1}. The results demonstrate that the fresh catalyst forms the active species via the reaction with hydrogen peroxide, and the active oxygen of the active species transfer to olefin in the epoxidation reaction, and subsequently the corresponding W–Ob–W (corner-sharing) and W–Oc–W (edge-sharing) bonds are formed.

In addition, in the ν(P–O) vibrational region, it is clear that the band at 1024 cm^{-1} gradually decreases in intensity and the band at 1125 cm^{-1} disappears, accompanying with the increase in the intensity of the band at 1079 cm^{-1} in the course of the reaction. Meanwhile, in the vibration regional (684–784 cm^{-1}) of the quaternary cation, the IR bands are quite distinctive, the broad bands at 684, 716 and 784 cm^{-1} gradually become sharp, suggesting that the interaction between the anion and the cation is changing in the reaction process.

When the insoluble fresh catalyst was treated with hydrogen peroxide in the absence of substrate, the ^{31}P NMR spectrum of the treated sample exhibits five peaks at 4.1, 0.3, −1.5, −2.3, and −12.1 ppm (see Fig. 4b). The lines at 4.3, 0.3, and −1.5 ppm can be attributed to $[(PO_4)\{WO(O_2)_2\}_4]^{3-}$, $[(PO_4)\{WO(O_2)_2\}_2\{WO(O_2)_2(H_2O)\}]^{3-}$, and $[(PO_3(OH))\{WO(O_2)_2\}_2]^{2-}$, respectively [26–30]. The results show that the catalyst depolymerizes into several smaller active species after it reacts with hydrogen peroxide. The peak at −2.3 ppm may be assigned to uncoordinated phosphate ion [27]. The peak at −12.1 ppm is characteristic of the compound with Keggin structure [44,45], which is formed after the catalyst loses some active oxygen when no further hydrogen peroxide is added. For the reaction system, ^{31}P NMR (Fig. 4c) is

similar to that in Fig. 4b, except that the peak at 0.3 ppm of the species $[(PO_4)\{WO(O_2)_2\}_2\{WO(O_2)_2(H_2O)\}]^{3-}$ disappears and a new peak at about −4.0 ppm appears. The results indicate that the $[(PO_4)\{WO(O_2)_2\}_4]^{3-}$, $[(PO_4)\{WO(O_2)_2\}_2\{WO(O_2)_2(H_2O)\}]^{3-}$, and $[(PO_3(OH))\{WO(O_2)_2\}_2]^{2-}$ peroxo complexes may transform each other during the course of the reaction [26–28].

On the basis of above results, it can be concluded that the W–Ob–W and W–Oc–W bonds of the fresh catalyst are broken and then the catalyst degrades into soluble species, $[(PO_4)\{WO(O_2)_2\}_4]^{3-}$, $[(PO_4)\{WO(O_2)_2\}_2\{WO(O_2)_2(H_2O)\}]^{3-}$, and $[(PO_3(OH))\{WO(O_2)_2\}_2]^{2-}$ while the catalyst reacts with hydrogen peroxide. These active species contain the common peroxo group $[W_2O_2(O_2)_4]$ [29]. The active species reacts with substrate and then the W–Ob–W and W–Oc–W bonds are formed after the active oxygen species are used up. The peroxo group $[W_2O_2(O_2)_4]$ can be regenerated via the reaction with hydrogen peroxide.

3.4. Characterization of the used catalyst

The used catalysts were characterized by FT-IR and ^{31}P MAS NMR. Fig. 3b presents the FT-IR spectra of the used catalyst. It can be seen that there are some differences in IR spectra between the fresh catalyst and the used one. It is found that the broad band at 1079 cm^{-1} of the fresh catalyst in the P–O regions turns into two bands at 1100 and 1045 cm^{-1}, whereas the band due to W=O vibration shifts from 935 to 950 cm^{-1}. A similar result was observed in the vibrational region of ν(W–Ob–W), where the band becomes from 884 to 863 and 895 cm^{-1}. In addition, the band at 813 cm^{-1} due to ν(W–Oc–W) markedly increases in intensity. But the band at 543 cm^{-1} disappears after the reaction. It is interesting that the IR bands of the used catalyst is in fair agreement with those of $[PW_{11}O_{39}]^{7-}$ with Keggin structure [43]. These assignments of the IR bands for the catalysts are listed in Table 2. ^{31}P MAS NMR spectrum of the used catalyst (Fig. 4d) reveals a single line at −12.6 ppm, which can be attributed to the lacunar Keggin-type structure of the $[PW_{11}O_{39}]^{7-}$ anion [43,44]. The results provide additional support for the IR spectra of used catalyst (Fig. 3), i.e., the active species, $[(PO_4)\{WO(O_2)_2\}_4]^{3-}$, $[(PO_4)\{WO(O_2)_2\}_2\{WO(O_2)_2(H_2O)\}]^{3-}$, and $[(PO_3(OH))\{WO(O_2)_2\}_2]^{2-}$ lose active oxygen and precipitate from the reaction solution and partly form $[PW_{11}O_{39}]^{7-}$ anion with Keggin structure after the reaction.

Table 2
Assignment of IR bands of the quaternary ammonium heteropolyoxotungstophosphates catalysts

IR bands (cm^{-1})	Assignment	References
1024–1125	ν(PO_4)	[16,26–30]
935, 944, 950	ν(W=O)	[16,26–30]
863, 884, 895	ν(W–Ob–W)	[43–45]
842	ν(O–O)	[16,26–30]
813	ν(W–Oc–W)	[43–45]
684–784	Quaternary cation	

As discussed above, it can be seen that the active species tends to transforms into more stable compounds with Keggin structure in the catalytic reaction cycles. Therefore, we prepared the fresh $[\pi\text{-}C_5H_5N(CH_2)_{15}CH_3]_7[PW_{11}O_{39}]$ and

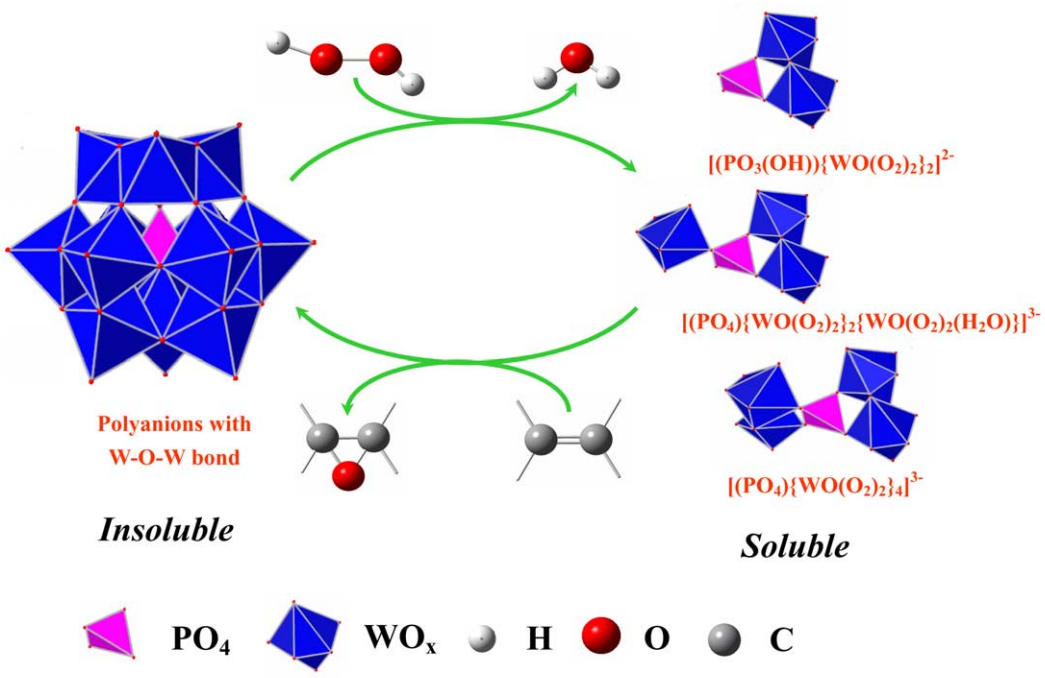

Scheme 1. Reaction mechanism of the reaction-controlled phase transfer catalysis for cyclohexene epoxidation.

$[\pi\text{-}C_5H_5N(CH_2)_{15}CH_3]_3[PW_{12}O_{40}]$ catalysts with Keggin structure by the procedure reported previously [20,28] and found that the catalysts also precipitates from the reaction medium after the epoxidation reaction. Furthermore, the ^{31}P MAS NMR spectrum of the used catalyst $[\pi\text{-}C_5H_5N(CH_2)_{15}CH_3]_3[PW_{12}O_{40}]$ (Fig. 4f) was analogous to that of the fresh $[\pi\text{-}C_5H_5N(CH_2)_{15}CH_3]_3[PW_{12}O_{40}]$ catalyst (Fig. 4e) except for the small broad peaks in the range of −10 to 10 ppm. The results indicate that the catalysts with Keggin structure can partly return to its original structure and precipitate from the reaction system after the epoxidation reaction. But the prepared catalysts with Keggin structure exhibits less catalytic efficiency than the $[\pi\text{-}C_5H_5N(CH_2)_{15}CH_3]_3[PW_4O_{16}]$ catalyst for epoxidation reaction. It took longer time for the catalysts with Keggin structure to dissolve into solvent. It seems that the compounds with higher P/W ratio were easier to reaction with hydrogen peroxide than the compounds with Keggin structure.

Based on above results, it can be concluded that the catalysts with Keggin-structural framework for both $[PW_{11}O_{39}]^{7-}$ and $[PW_{12}O_{40}]^{3-}$ have the reaction-controlled phase transfer property at least under the reaction conditions of cyclohexene epoxidation with 35% H_2O_2 and $CHCl_3$ solvent. The Keggin-type precursors have been investigated as the catalysts of epoxidation by many groups [26–30], Hill and co-workers [28] and Griffith and co-workers [30] reported that the $[PW_{12}O_{40}]^{3-}$ and its lacunary derivative $[PW_{11}O_{39}]^{7-}$ can also form smaller active species $[(PO_4)\{WO(O_2)_2\}_4]^{3-}$, $[(PO_4)\{WO(O_2)_2\}_2\{WO(O_2)_2(H_2O)\}]^{3-}$, and $[(PO_3(OH))\{WO(O_2)_2\}_2]^{2-}$ in the presence of hydrogen peroxide. We found that the smaller species lose the active oxygen after the epoxidation reaction and polymerize into larger compounds by forming the W–Ob–W and W–Oc–W bonds, and then precipitate from the reaction system after the hydrogen peroxide is consumed up. The reaction-controlled phase transfer is essential a process of degradation and polymerization of the catalyst anions. The mechanism for the reaction-controlled phase transfer catalyst can be described as in Scheme 1.

4. Conclusions

A conversion of about 90% and a selectivity of over 90% were obtained for epoxidation of cyclohexene with H_2O_2 (35%) on a reaction-controlled phase transfer catalyst composed of quaternary ammonium heteropolyoxotungstates, $[\pi\text{-}C_5H_5N(CH_2)_{15}CH_3]_3[PW_4O_{16}]$. The fresh catalyst is insoluble but becomes soluble when it reacts with hydrogen peroxide and precipitates again when the epoxidation reaction is over. The catalysts and the fresh catalyst under reaction conditions were characterized by FT-IR, Raman and ^{31}P NMR spectroscopy, it is found that the fresh catalyst $[\pi\text{-}C_5H_5N(CH_2)_{15}CH_3]_3[PW_4O_{16}]$ is a complex mixture, which can form smaller active species $[(PO_4)\{WO(O_2)_2\}_4]^{3-}$, $[(PO_4)\{WO(O_2)_2\}_2\{WO(O_2)_2(H_2O)\}]^{3-}$, and $[(PO_3(OH))\{WO(O_2)_2\}_2]^{2-}$ via the reaction with hydrogen peroxide. After the hydrogen peroxide is used up, these smaller anions polymerize into larger anions with forming the W–Ob–W and W–Oc–W bonds, as a result, the catalyst becomes insoluble solid and precipitates from the reaction medium.

Acknowledgements

This work was partly supported by the Natural Science Foundation of China (Grant Nos. 20233050 and 20073045). Jinbo Gao thanks professor Yi Chi for his help.

References

[1] M.T. Pope, Heteropoly and Isopoly Oxometalates, Springer-Verlag, Berlin, 1983.
[2] M.T. Pope, A. Müller, Angew. Chem. Int. Ed. Engl. 30 (1991) 34.
[3] V.W. Day, W.G. Klemperer, Science 288 (1985) 533.
[4] C.L. Hill, Activation and Functionalization of Alkanes, Wiley, New York, 1989, pp. 243–279.
[5] C.L. Hill, R.B. Brown Jr., J. Am. Chem. Soc. 108 (1986) 536.
[6] X. Zhang, Q. Chen, D.C. Duncan, C.F. Campana, C.L. Hill, Inorg. Chem. 36 (1997) 4208.
[7] X. Zhang, T.M. Anderson, Q. Chen, C.L. Hill, Inorg. Chem. 40 (2001) 418.
[8] A.C. Dengel, W.P. Griffith, R.D. Powell, A.C. Skapski, J. Chem. Soc., Chem. Commun. 7 (1986) 555.
[9] N.J. Campbell, A.C. Dengel, C.J. Edwards, W.P. Griffith, J. Chem. Soc., Dalton Trans. (1989) 1203.
[10] A.C. Dengel, W.P. Griffith, B.C. Parkin, J. Chem. Soc., Dalton Trans. (1993) 2683.
[11] A.J. Bailey, W.P. Griffith, B.C. Parkin, J. Chem. Soc., Dalton Trans. (1995) 1833.
[12] W.P. Griffith, B.C. Parkin, A.J.P. White, D.J. Williams, J. Chem. Soc., Dalton Trans. (1995) 3131.
[13] C. Venturello, E. Alneri, M. Ricci, J. Org. Chem. 48 (1983) 3831.
[14] C. Venturello, R. D'Aloisio, J.C. Bart, M. Riai, J. Mol. Catal. 32 (1985) 107.
[15] C. Venturello, M. Ricci, J. Org. Chem. 51 (1986) 1599.
[16] C. Venturello, R. D'Aloisio, J. Org. Chem. 53 (1988) 1553.
[17] C. Venturello, M. Gambaro, Synthesis 4 (1989) 295.
[18] P. Fantucci, S. Lolli, C. Venturello, J. Catal. 169 (1997) 228.
[19] Y. Ishii, K. Yamawaki, T. Yoshida, T. Ura, H. Yamada, M. Ogawe, J. Org. Chem. 52 (1987) 1868.
[20] Y. Ishii, K. Yamawaki, T. Ura, H. Yamada, T. Yoshida, M. Ogawe, J. Org. Chem. 53 (1988) 3587.
[21] S. Sakaue, Y. Sakata, Y. Nishiyama, Y. Ishii, Chem. Lett. 2 (1992) 289.
[22] S. Sakaue, T. Tsubakino, Y. Nishiyama, Y. Ishii, J. Org. Chem. 58 (1993) 3633.
[23] Y. Ishii, H. Tanaka, Y. Nishiyama, Chem. Lett. 1 (1994) 1–4.
[24] K. Nakayama, M. Hamamoto, Y. Nishiyama, Y. Ishii, Chem. Lett. 10 (1993) 1699.
[25] M. Hamamoto, K. Nakayama, Y. Nishiyama, Y. Ishii, J. Org. Chem. 58 (1993) 6421.
[26] C. Aubry, G. Chottard, N. Platzer, J.M. Brégeault, R. Thouvenot, F. Chaureau, C. Huet, H. Ledon, Inorg. Chem. 30 (1991) 4409.
[27] L. Sales, C. Aubry, R. Thouvenot, F. Robert, C.D. Morin, G. Chottard, H. Ledon, Y. Jeannin, J.M. Brégeault, Inorg. Chem. 33 (1994) 871.

[28] D.C. Duncan, R.C. Chambers, E. Hecht, C.L. Hill, J. Am. Chem. Soc. 117 (1995) 681.
[29] L. Salles, J.Y. Piquemal, R. Thouvenot, C. Minot, J.M. Brégeault, J. Mol. Catal. 117 (1997) 375.
[30] N.M. Grecley, W.P. Griffith, A.C. Laemmel, H.S. Nogueira, B.C. Parkin, J. Mol. Catal. 117 (1997) 185.
[31] R. Neumann, M. Gara, J. Am. Chem. Soc. 116 (1994) 5509.
[32] R. Neumann, M. Gara, J. Am. Chem. Soc. 117 (1995) 5066.
[33] R. Neumann, M. Dahan, Nature 388 (1997) 353.
[34] C.L. Hill, X. Zhang, Nature 373 (1995) 324.
[35] K. Sato, M. Aoki, M. Ogawa, T. Hashimoto, R. Noyori, J. Org. Chem. 61 (1996) 8310.
[36] T. Yamase, E. Ishikawa, Y. Asai, S. Kanai, J. Mol. Catal. A 114 (1996) 237.
[37] Y. Sun, Z. Xi, G. Cao, J. Mol. Catal. 166 (2001) 219.
[38] Z. Xi, N. Zhou, Y. Sun, K. Li, Science 292 (2001) 1139.
[39] L.J. Csányi, K. Jáky, J. Mol. Catal. 61 (1990) 75.
[40] L.J. Csányi, K. Jáky, J. Catal. 127 (1991) 42.
[41] C. Li, G. Xiong, Angew. Chem. Int. Ed. Engl. 38 (1999) 2220.
[42] C. Li, G. Xiong, J. Phys. Chem. B 105 (2001) 2993.
[43] E. Radkov, R.H. Beer, Polyhedron 14 (1995) 2139.
[44] N.I. Kuznetsova, L.G. Detusheva, L.I. Kuznetsova, M.A. Fedotov, V.A. Likholobov, J. Mol. Catal. 114 (1996) 131.
[45] L.R. Pizzio, C.V. Cáceres, M.N. Blanco, Appl. Surf. Sci. 151 (1999) 91.